Surface and Interfacial FT–IR Spectroscopic Studies of Latexes. VI. Orientation and Spatial Distribution of Acid Functionalities at the Film–Substrate Interface

TIMOTHY A. THORSTENSON, LARA K. TEBELIUS, and MAREK W. URBAN*

Department of Polymers and Coatings, North Dakota State University, Fargo, North Dakota 58105

SYNOPSIS

Formation of dimeric carboxylic acid functional groups observed at the film-substrate interface of ethyl acrylate/methacrylic acid (EA/MAA) and butyl acrylate/methyl methacrylate/methacrylic acid (BA/MMA/MAA) latex films prepared on a high surface tension substrate, such as liquid mercury, is observed when sodium dioctyl sulfosuccinate (SDOSS) is employed as the synthetic emulsifier. To address the acid species assembled at this interface due to the inability of SDOSS to effectively alleviate interfacial tension and to assess the orientation and spatial configuration of acid groups species at the interface, polarized attenuated total reflectance, Fourier-transform infrared spectroscopy (ATR FT-IR) is employed. It is found that the acid dimer rings adopt an average "on-edge" configuration at the interface with the hydrogen-bonded rings perpendicular to the film–mercury interface. This configuration serves to provide not only the necessary interfacial acid-dimer layer, but also facilitates favorable ring–ring interactions between groups of opposite polarity on adjacent rings. This study indicates that the on-edge configuration may also serve to reduce unfavorable interactions between the polar acid functionality and the less polar components present in the bulk of the coalesced latexes. © 1993 John Wiley & Sons, Inc.

INTRODUCTION

The interactions between surfactants and latex components, along with the factors influencing surfactant mobility represent critical issues in latexes since their magnitude may influence ultimate macroscopic film characteristics. Previously, we have identified several variables that may affect surfactant mobility and dynamics of migration.[1-7] They include substrate surface tension and mechanical deformation,[3] surfactant and copolymer structures,[4,5] and hydrophobic surfactant–copolymer interactions.[4,5] The nature of interactions between sodium dioctyl sulfosuccinate (SDOSS) and sodium dodecylbenzene sulfonate (SDBS) surfactants and the acid groups of the copolymer latex have been addressed.[6,7] These studies showed that the surfactants, because of their highly polar sulfonate groups,

can form hydrogen-bonded structures with both the copolymer acid functionality and with residual water present in the coalesced latex film. The position of the equilibrium between hydrated and acid-bonded surfactant groups is affected by the concentration of atmospheric water vapor present during and after film formation.[7]

Although these studies provided considerable insights into the nature of these interactions, an assessment of the spatial distribution and orientation of the latex system components yields more information concerning the magnitude of these interactions. This issue is particularly relevant in view of the previous studies[5] where the magnitude of anionic surfactant enrichment to the film–substrate (F–S) interface of butyl acrylate/methyl methacrylate/methacrylic acid (BA/MMA/MAA) latex films was reduced relative to ethyl acrylate/methacrylic acid (EA/MAA) films. This behavior is believed to be caused by the presence of the longer hydrophobic butyl groups that may facilitate latex–surfactant interactions via two mechanisms:

---

1. enhanced surfactant/copolymer compatibility brought about by the greater potential for hydrophobic interactions; and

2. alleviation of film–substrate interfacial tension caused by the presence of the longer butyl groups that, relative to ethyl groups, may be more able to orient toward low surface-tension substrates such as polytetrafluoro-ethylene (PTFE).

Additionally, it has been observed that, in the case of latexes prepared with sodium dioctyl sulfosuccinate (SDOSS) surfactant, considerable quantities of dimeric carboxylic acid species may assemble at the F–S interface when latex films were prepared on liquid mercury.[3] This phenomenon was attributed to the ineffectiveness of SDOSS to compensate for interfacial tension present at the interface and the suggestion that the acid dimer functionality may provide a higher surface-tension film interface that the mercury can more readily wet. Because orientation or the distribution of orientations in a preferred direction may provide constructive or destructive contribution to macroscopic properties, their orientation near the film–air (F–A) and F–S interfaces of the coalesced films is of primary importance. In addition to the issue of compatibility, it is also desirable to obtain further information regarding the nature of the hydrogen-bonding interactions, namely, the previously reported[3] acid dimer interactions. Here, we expand the scope of the previous studies and try to assess the orientation and distribution of the acid dimer rings at the F–S interface of films prepared on high surface-tension liquid mercury surfaces. An ultimate goal is to determine if these interactions serve to induce possible preferential molecular level orientations by "freezing" the copolymer segments into a defined spatial configuration at the F–S interface.

EXPERIMENTAL

Synthesis of EA/MAA and BA/MMA/MAA latexes with SDOSS surfactant was reported earlier.[5,6] All latexes were synthesized to maintain a 4.0 w/w % MAA concentration and a 4.0 w/w % surfactant concentration (based on monomer weight). As reported previously,[6] approximately 100-μ thick latex films were prepared on PTFE and liquid mercury and allowed to coalesce under ambient conditions for 72 h prior to spectral acquisition. After coalescence, the films were removed from the substrates

and the F–A and F–S interfaces were examined using ATR FT–IR spectroscopy.

ATR FT–IR spectra were recorded on a Digilab FTS-20 equipped with a variable angle rectangular ATR attachment (Spectra Tech). In a typical experiment, 200 coadded scans were acquired and ratioed against an appropriate background. Polarization of the IR radiation was accomplished with a Specac 12000 IR polarizer placed in the beam path and adjusted to obtain the desired polarization.

RESULTS AND DISCUSSION

Before discussing the results of ATR FT–IR experiments using polarized infrared light, it is appropriate to define the experimental setup. Figure 1 shows a typical rectangular ATR assembly used for polarized radiation experiments.[8] The crystal plane is defined in terms of the x and y axes while the z axis is perpendicular to the x, y plane. Following the accepted convention,[9] the transverse electric (TE) wave is defined as having its electric vector parallel to the crystal plane (or perpendicular to the plane of incidence), whereas the transverse magnetic (TM) polarization has an electric vector perpendicular to the crystal plane. It should be noted that there is a significant difference in experimental considerations between this study and the studies performed using the polarized ATR FT–IR setup to examine orientation of polymer chains or changes induced by mechanical processing.[8,10] In those experiments, it was necessary to differentiate between the x and y directions (Fig. 1) by rotating the sample or crystal so that preferential orientation with respect to the direction of drawing or processing could be identified. In our case, however, we deal with amorphous polymers and the primary concern is differentiation between groups aligned parallel or perpendicular to the film plane surface. Therefore, it is not necessary to change the sample position with respect to the ATR crystal, especially considering the fact that, during film formation and sample preparation, there are no identified driving forces inducing preferential orientation within the plane.

With these considerations in mind, let us focus on EA/MAA/SDOSS films prepared on liquid mercury as the substrate of choice because of its high surface tension. We have already shown that the migration of SDOSS surfactant to the F–S interface is accompanied by the assembly of a considerable quantity of carboxylic acid functionalities.[3] Migration of the latter species results in the presence
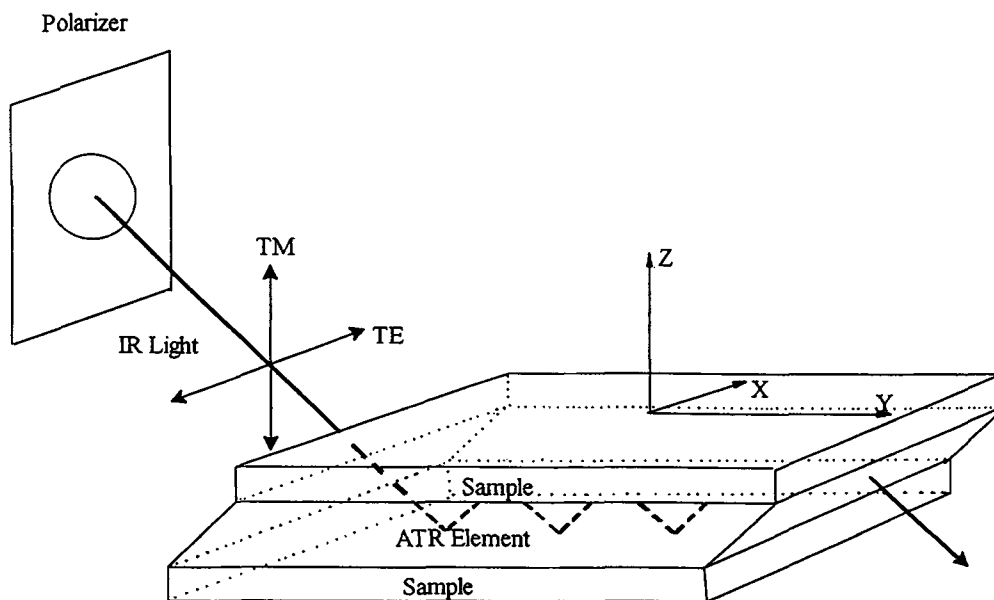
Figure 1   Schematic diagram of an ATR FT–IR experimental setup for use with polarized infrared light.

of the 938 cm^{-1} O — H $\cdot$ $\cdot$ O out-of-plane deformation mode and the bands at 664, 650, 598, and 575 cm^{-1}, tentatively attributed to the O — CO in-plane deformation normal modes. Although these studies suggested that the carboxylic acid species have a tendency to migrate to the F–S interface because of the ineffectiveness of SDOSS in alleviating the interfacial tension present between the latex film and the Hg substrate, their orientation and arrangements are yet to be understood.

With this in mind, let us now consider the results of polarization experiments. Figure 2 shows the 970–530 cm^{-1} region of the spectra collected at the F–S interface of the films prepared on Hg. Trace A is the TE spectrum, whereas trace B is its TM counterpart. In contrast to the F–A interface spectra (not shown), several bands show intensity changes attributed to orientation effects. For example, the 938 cm^{-1} band caused by the O — H $\cdot$ $\cdot$ O out-of-plane deformation mode reveals strong enhancement with TE polarization. Additionally, the bands at 650, 598, and 575 cm^{-1} also exhibit fairly pronounced polarization dependance.

Temporarily postponing further polarization data analysis, it is appropriate to address the band assignments. The assignment of the band at 938 cm^{-1} (Fig. 2) is quite straightforward (OH $\cdot$ $\cdot$ O out-of-plane deformation of the carboxylic acid dimers).[4] The three bands at 650, 598, and 575 cm^{-1}, however, require further considerations. Based on the band

assignments obtained in the studies of organic acids and other similar compounds,[11] the presence of the three bands in the 665–610 cm^{-1} region is attributed to the O — CO in-plane normal deformation modes
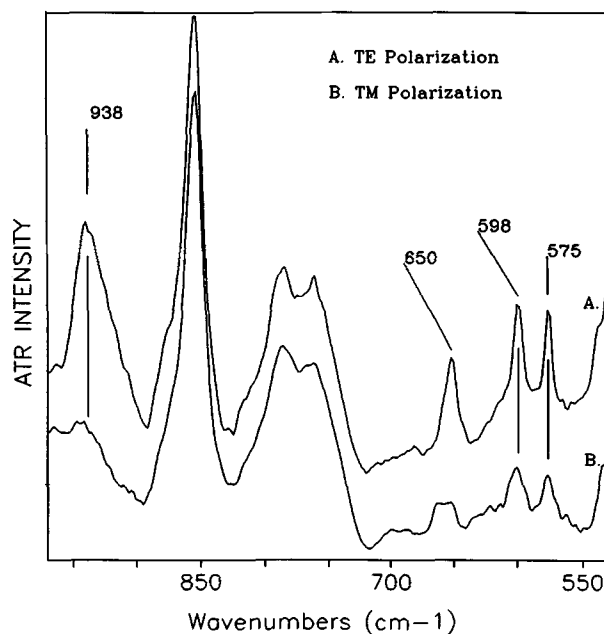
Figure 2   Polarized ATR FT–IR spectra in the 970–530 cm^{-1} region recorded at the F–S interface of an EA/MAA/SDOSS latex film prepared on liquid mercury. (A) TE polarization and (B) TM polarization.

caused by carboxylic acid dimers. Although the above assignments seem to agree with the literature considerations, several significant differences between the latex system and the low molecular weight model acid compounds used in developing these assignments should be pointed out. First, the acid functionality present in the latex system is of a polymeric nature and the substituent groups attached to the COOH moieties are of very high molecular weight. This factor may lead to variations in the vibrational frequencies observed for these modes. Additionally, conformational restrictions on the acid groups imposed by attachment to the polymer chains and the highly ordered manner in which these species apparently assemble at the mercury interface may also influence the vibrational frequency, and perhaps the infrared intensity.

Let us note that the 650 cm^{-1} band shows considerable intensity in the TE polarized spectrum (Fig. 2, trace A). Although the vibrational energy of this band agrees with the literature, our assignment is complicated by the fact that the surfactant also exhibits a band caused by the S—O bending mode of SO_3 in the same region. Further insights into the nature of this band can be revealed by considering the similarly positioned band shown in trace C of Figure 3. This spectrum is the nonpolarized
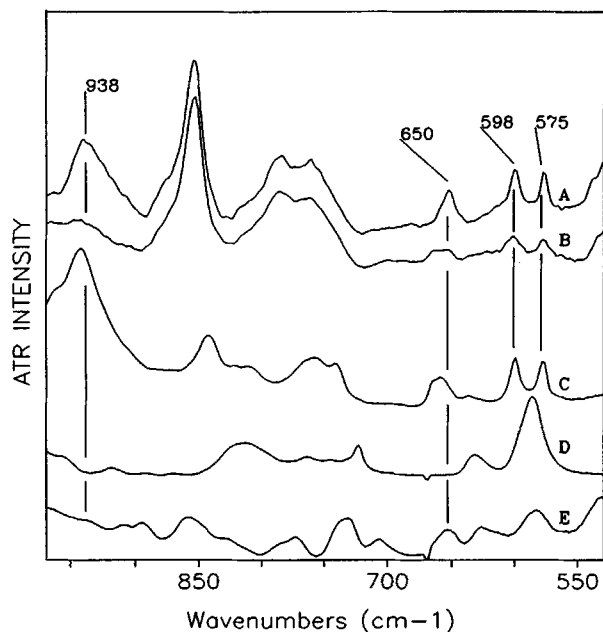

Figure 3   ATR FT–IR spectra in the 970–530 cm^{-1} recorded at the F–S interface of latex films prepared on liquid mercury. (A) EA/MAA/SDOSS (TE polarization); (B) EA/MAA/SDOSS (TM polarization); (C) BA/MMA/MAA/SDS (no polarization); (D) neat SDS surfactant; (E) neat SDOSS surfactant.

ATR FT–IR spectrum of a BA/MMA/MAA latex prepared using sodium dodecyl sulfate (SDS) surfactant. Because of enhanced intensities of the bands at 938, 598, and 575 cm^{-1}, this latex also exhibits enrichment of the acid functionality at the F–S interface and, although the SDS spectrum reveals no bands in the 650 cm^{-1} region (trace D), the 650 cm^{-1} band is clearly absent. Based on this result and the observed polarization dependance of the 650, 598, and 575 cm^{-1} bands, these bands are attributed to the O—CO in-plane deformation modes.

At this point, let us go back to the main theme and establish the distribution of acid functionality at the latex interfaces. In order to do so, it is first necessary to correlate the acid-dimer structure with the band intensities and their polarization dependance. While structure A of Figure 4 shows a typical acid-dimer structure, there are two vibrational modes that require further considerations: (1) out-of-plane deformation mode of the O—H···O groups, and (2) the in-plane O—CO deformation modes. Structure B of Figure 4 shows an "edge" view of the dimer ring. As shown by arrows, the dipole moment changes during this normal deformation mode lie perpendicular to the ring plane. In contrast, the O—CO deformation is an in-plane mode with the dipole moment changes lying in the ring plane. This is illustrated in structure C of Figure 4.

Having established the orientation of the dipole moment changes associated with the acid-dimer deformation modes, the spatial orientation of these groups may be assessed. This is accomplished by considering the possible configurations of these groups in the context of the experimental polarization data. Figure 5 illustrates five major structural possibilities in which the individual acid-dimer groups may be configured at the F–S interface. While structure A of Figure 5 shows the acid-dimer group situated in the film plane with the ring parallel to the F–S interface, structures B and C illustrate two other alternatives for a ring structure to be perpendicular to the film plane. In addition to these orientations, the structures such as the ones designated D-1 and D-2 (Fig. 5) may occur. Structure D-1 accounts for a significant deviation from the planar ring structure with one acid group predominantly in-plane and the other perpendicular or randomly oriented with respect to the film plane. In contrast, structure D-2 represents one acid group perpendicular to the plane and the other group parallel or randomly oriented, complementing structure D-1. Although we realize that there may be many structures that can be conceived of in which the dimers do not form a planar structure and the individual
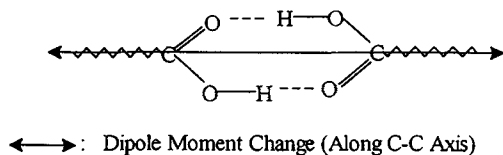
A. Typical Acid Dimer Structure
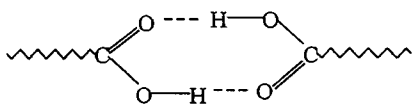
B. Representation of O - - - H-O Out-Of-Plane Deformation

←——→ : Dipole Moment Change (Perpendicular To Ring Plane)
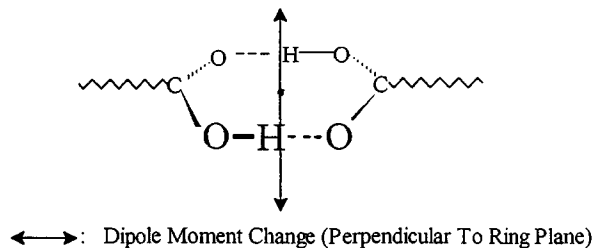
C. Representation of O-CO In-Plane Deformations

←——→ : Dipole Moment Change (Along C-C Axis)

Figure 4 Typical acid dimers and their normal vibrational modes of interest. (A) Acid-dimer structure; (B) representation of the dipole moment change during the OH˙˙˙O out-of-plane ring deformation observed at 938 cm^{-1}; (C) representation of dipole moment change during the O — CO in-plane ring deformations observed at 650, 598, and 575 cm^{-1}.

acid groups lie at a certain angle with respect to each other and with respect to the film plane, Figure 5 illustrates only representative examples.

To identify the most feasible structure that is in agreement with the experimental data presented in Figure 2, let us first consider the O — H · · · O deformation modes of the dimer ring. As we indicated above, the dipole moment changes of these modes lie perpendicular to the dimer-ring plane (Fig. 4, structure B). This mode corresponds to the 938 cm^{-1} absorbance in the ATR spectrum and, according to trace A of Figure 2, it is significantly enhanced with TE polarization. This result suggests the presence of a localized structure such as that shown in struc-

tures B and C of Figure 5 and tends to rule out in-plane ring assembly illustrated by structure A since such a configuration would lead to the TM enhancement of the 938 cm^{-1} mode.

Further insight about the dimer-ring orientation may be obtained by considering the in-plane O — CO modes at 650, 598, and 575 cm^{-1}. Referring again to Figure 2, these bands also reveal significant enhancement for TE polarization (trace A), indicating that the displacement vectors associated with the dipole moment changes of these deformation modes should lie in the F–S plane. Although this result does not allow us to differentiate between in-plane and out-of-plane ring positioning, it can be used to differentiate between structures B and C of Figure 5. According to the band intensity changes, these dipole moments ought to lie predominantly in-plane, favoring structure B over structure C. A similar argument can be used to rule out the presence of structure D-1, favoring again partial "on-edge" configuration depicted in D-2.

Although these results suggest that the dominating structural feature are the structures B and D-2 of Figure 5, it is still necessary to address the longer-range order of these interfacial species and to identify as to why this on-edge conformation is adopted in preference to one that places the rings parallel to the interface. To address this issue, let us first examine the results of the depth profiling experiments performed on the EA/MAA/SDOSS films we have discussed above. While Figure 6 shows the TE polarized spectra acquired by varying the nominal ATR angle of the KRS-5 element from 60° to 40° in 5° increments (Traces A through E, respectively), Figure 7 shows the corresponding TM polarized spectra. This depth profiling provides a variation of the depth of penetration (d_p) from approximately 1.16 to 1.54 μ at 1000 cm^{-1}, with the reference point at the film–crystal contact that, in this case, is the F–S interface. Evidently, a consistent trend of the increasing acid-dimer band intensity is observed with the increasing ATR angle and no significant changes in relative orientation are observed as the surface is probed deeper. These observations suggest that the acid-dimer functionality is indeed assembled in a highly ordered fashion at and near the film–mercury interface.

Our previous studies have shown[5] that latex copolymer structure may exert significant influence on interfacial behavior and that it is worthwhile to examine the behavior of the acid-dimer species assembled at the F–S interface of BA/MMA/MAA/SDOSS latex films prepared on mercury. Figure 8 shows the TE (trace A) and TM (trace B) polar-
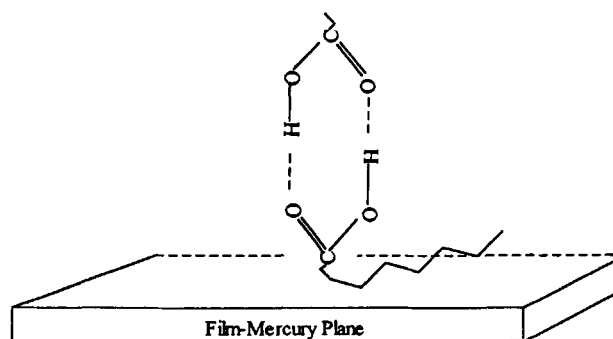
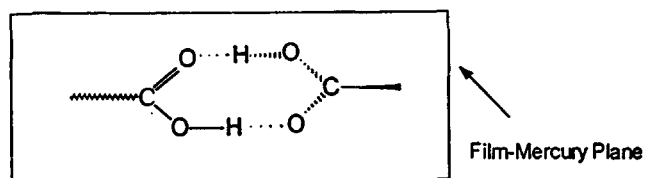Schematic Depiction of Possible Local Dimer Orientations

A. Ring In Film Plane

Film-Mercury Plane
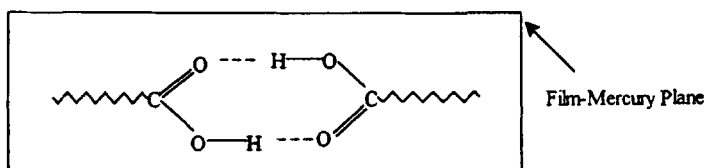
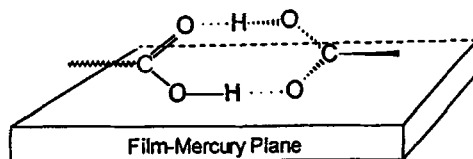B. Ring Perpendicular To Film Plane (C-C Axis In Plane)

Film-Mercury Plane
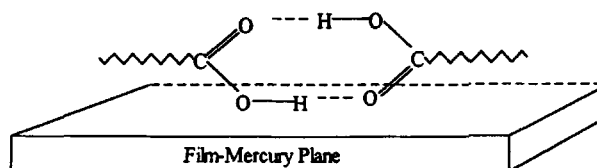
C. Ring Perpendicular To Film Plane (C-C Axis Perpendicular To Plane)

Film-Mercury Plane

D-1 . Non-Planar Structure

Film-Mercury Plane
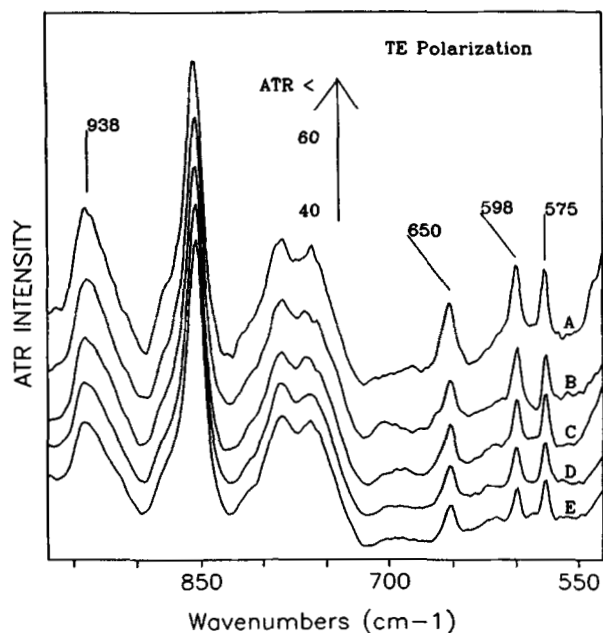
D-2 . Non-Planar Structure

Film-Mercury Plane

Figure 5   Possible local acid-dimer ring orientations. (A) Ring situated in film plane; (B) ring perpendicular to film plane (ring C–C axis in film plane); (C) ring perpendicular to film plane (ring C–C axis perpendicular to film plane); (D) example of possible nonplanar ring structures.
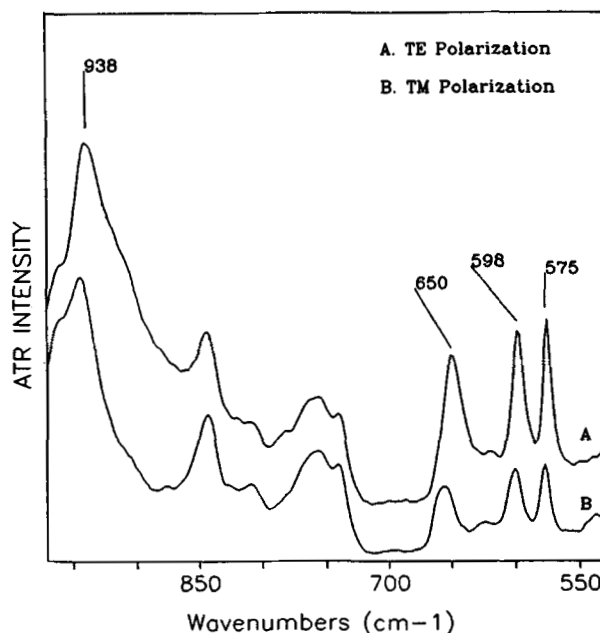
Figure 6 TE polarized ATR FT–IR spectra in the 970–530 cm^{-1} region recorded as a function of ATR angle at the F–S interface of an EA/MAA/SDOSS latex film prepared on liquid mercury. (A) 60°; (B) 55°; (C) 50°; (D) 45°; (E) 40°.

izations of spectra acquired at a 60° ATR angle. Once again, the familiar bands at 938, 650, 598, and 575 cm^{-1} caused by normal deformation modes of
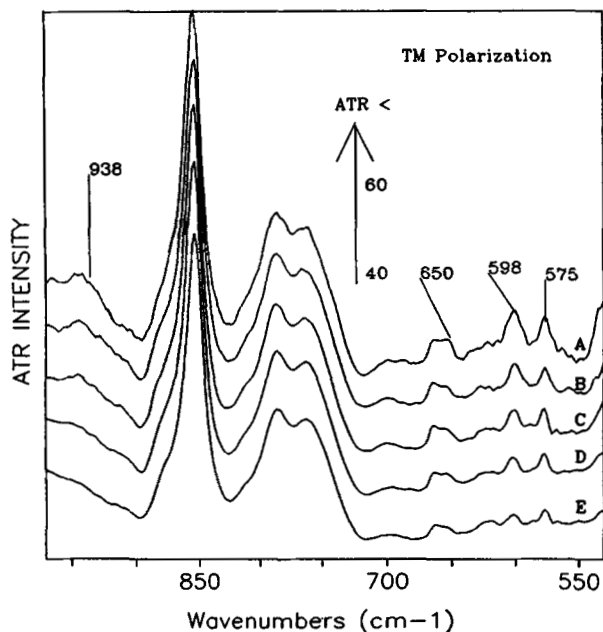
Figure 7 TM polarized ATR FT–IR spectra in the 970–530 cm^{-1} region recorded as a function of ATR angle at the F–S interface of an EA/MAA/SDOSS latex film prepared on liquid mercury. (A) 60°; (B) 55°; (C) 50°; (D) 45°; (E) 40°.

Figure 8 Polarized ATR FT–IR spectra in the 970–530 cm^{-1} region recorded at the F–S interface of a BA/MMA/MAA/SDOSS latex film prepared on liquid mercury. (A) TE polarization; (B) TM polarization.

the acid-dimer groups are observed. The same qualitative polarization dependance that was observed for the EA/MAA/SDOSS system is demonstrated. Similarly to the EA/MAA/SDOSS system, depth-profiling results (not shown) reveal a consistent decrease in acid-dimer band intensity as greater film depths are probed. No detectable changes in the composition of the rest of the copolymer are detected by changing the ATR angle. This observation suggests that the interfacial dimeric species assemble at the interface between the mercury surface and an otherwise relatively homogeneous copolymer whose composition does not apparently yield significant influence on the nature of the dimer assembly. Furthermore, now we are in a position to propose reasons for the observed spatial configuration of acid-dimer functionality and to identify the nature of the longer-range order of the species at the interface. To address these issues, let us establish why the acid-dimer rings observed at the F–S interface adopt the on-edge configuration. Conceptually, one would expect a flat, in-plane configuration to be most likely present. The on-edge assembly seems especially puzzling in light of the fact that the very reason the dimeric species are induced to assemble at the interface is apparently in order to alleviate Hg/copolymer interfacial tension. Based on this rationale, in-plane ring assembly would appear to be the more reasonable configuration since it would seemingly provide for more efficient coverage of the interface

and more effective interaction with the mercury. The on-edge orientation, however, may be readily explained by considering not only the mercury–dimer interactions, but also the potential for ring–ring interactions between groups of opposing polarity on adjacent rings. Their presence in a long-array dimer assembly may occur, providing there is a sufficient number of dimers for adequate surface-area coverage. An assembly of this nature facilitates not only the desired dimer–mercury interactions but, it also provides for an abundance of favorable ring–ring interactions. In addition to these factors, it is also possible that this spatial configuration serves to reduce the magnitude of unfavorable interactions between the polar-dimer rings and the less polar segments of the copolymer.

CONCLUSIONS

Orientation and longer range spatial order of dimeric carboxylic acid species that assemble at the interface between latex films and a liquid mercury substrate in order to alleviate interfacial free energy have been assessed. These studies suggest that these dimeric species assemble in an on-edge configuration at the interface and this type of configuration appears to be most favorable because it accounts not only for the dimer–mercury interactions but it also facilitates favorable interactions between groups of opposite polarity on adjacent dimer rings. Additionally, it is possible that the on-edge assembly may serve to minimize unfavorable interactions between the acid-dimer functionality and the less polar copolymer components present in the bulk of the film.

REFERENCES

1. M. W. Urban and K. W. Evanson, *Polym. Commun.,* **31,** 279–282 (1990).
2. K. W. Evanson and M. W. Urban, in *Surface Phenomena and Fine Particles in Water-Based Coatings and Printing Technology,* M. K. Sharma and F. J. Micale, Eds., Plenum Press, New York, 1991.
3. K. W. Evanson and M. W. Urban, *J. Appl. Polym. Sci.,* **42,** 2309–2320 (1991).
4. K. W. Evanson, T. A. Thorstenson, and M. W. Urban, *J. Appl. Polym. Sci.,* **42,** 2297–2307 (1991).
5. T. A. Thorstenson and M. W. Urban, *J. Appl. Polym. Sci.,* to appear.
6. K. W. Evanson and M. W. Urban, *J. Appl. Polym. Sci.,* **42,** 2287–2296 (1991).
7. T. A. Thorstenson and M. W. Urban, *J. Appl. Polym. Sci.,* to appear.
8. C. S. P. Sung, *Macromolecules,* **14,** 591–594 (1981).
9. P. A. Fluornoy and W. J. Schaffers, *Spectrochim. Acta,* **22,** 5 (1966).
10. J. P. Hobbs, C. S. P. Sung, K. Krishnan, and S. Hill, *Macromolecules,* **16,** 193–199 (1983).
11. G. Socrates, *Infrared Characteristic Group Frequencies,* Wiley–Interscience, New York, 1980, pp. 64–66.